

Mass and charge distribution analysis in Negative Electrosprays of large polyethylene glycol chains by Ion Mobility Mass Spectrometry (NESI-IMS-MS)

Ernesto Criado-Hidalgo^{1,2}, Juan Fernández-García¹, Juan Fernández de la Mora^{1,a}

¹*Yale University-Mechanical Engineering Dept., New Haven, CT;*

²*SEADM, Boecillo, Spain*

^a Corresponding author; juan.delamora@yale.edu

SUPPORTING INFORMATION

This section discusses the following points: 1. Low z acquired by chains unable to bind ions. 2. Charge state and shape assignment from mobility data. 3. Analysis of narrow mass distribution PEG 12.6k. 4. Multiple conformers. 5. Charging probability at low z captured with PEG 6k. 6. More on the ionization mechanism. 7. DMA-MS analysis at reduced PEG concentration. 8. Study of a sample of PEG 2k.

SI.1. Low z acquired by chains unable to bind ions

One possible strategy to limit the charge on the gas phase polymer ion is to identify solution ions that bind considerably more weakly (or not at all) to the polar groups in the chain. Figure SI1 is an example of a two-dimensional IMS-MS positive ESI spectrum of a sample of Psty with a narrow mass distribution centered at ~ 9 kDa. Ion abundance is given in a logarithmic color scale, and the various charge states z and levels of aggregation n of the ions produced from the relatively concentrated Psty solution are indicated in the form n^{+z} . The horizontal variable is inversely proportional to ion mobility and the vertical scale is m/z in Da. For reference, a typical PEG ion of 9 kDa would take up to about 18 charges, while a Psty ion of the same mass carries primarily one, with a small proportion of doubly charged ions 1^{+2} also present.

Cleanly electrospraying high mass Psty is difficult,²² so the charging characteristics of electrosprayed Psty will be discussed elsewhere. The relevant point here is that the absence of polar groups in the Psty backbone limits the attachment of solution ions to it, confirming the notion that, without a strong chain-ion binding, only globular ions tend to form.

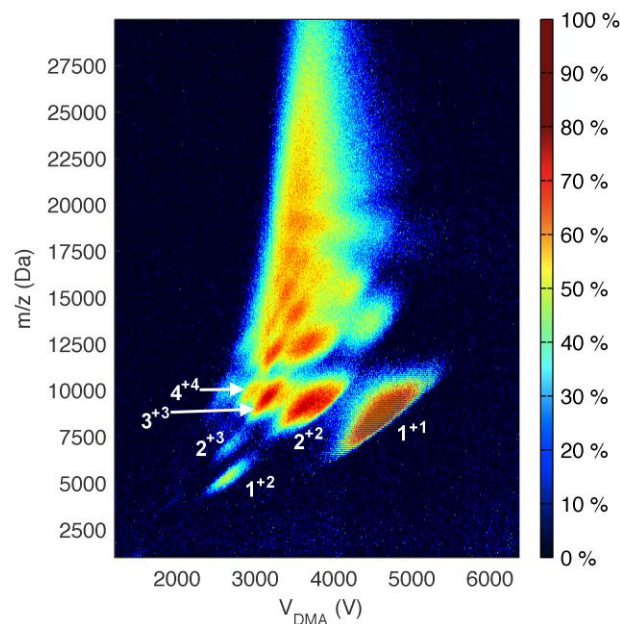


Figure SI1: Narrow mass distribution sample of Psty 9.2k, 300 μ M sprayed in the positive mode in a buffer of 30mM dimethylammonium formate (Met₂AF) in 1-Methyl-2-Pyrrolidone (NMP)-Dimethylformamide (DMF) 50:50 vol.

SI.2. Charge state and shape assignment from mobility data

Additional confirmation of both the correct z assignment made and the globular shape has been previously demonstrated by converting the ion mass m and the collision cross section ($\Omega \sim z/Z$) into the corresponding mass diameter $d_m = [6m/(\pi\rho)]^{1/3}$ and mobility diameter d (defined in equations SI-1-2 below) of a sphere,³² using the published value for the density of PEG [$\rho = 1.115 \text{ g/cm}^3$].³³ The approach is improved here to correct for the decrease in mobility associated to the extra attraction between the ion and the dipole it induces in the bath gas, given by (SI-1-3):

$$Z = Z_o (1 - \beta \varepsilon^*) \quad (\text{SI-1})$$

$$Z_o = 0.44 \frac{ze}{pd^2} \left(\frac{kT}{\mu} \right)^{1/2}, \quad \varepsilon^* = 2\alpha e^2 z^2 / [\pi \varepsilon_o k T d^4], \quad (\text{SI-2,3})$$

³² Larriba, C.; Hogan Jr., C. J.; Attoui, M.; Borrajo, R.; Fernandez Garcia, J.; Fernandez de la Mora, J. *The Mobility-Volume Relationship below 3.0 nm examined by Tandem Mobility-Mass Measurement, Aerosol Sci. Technol.* **2011**, 45: 4, 453-467.

³³ Mark, J. E. *Polymer Data Handbook*; Oxford University Press: New York, 1999.

where Z_o is the mobility in the absence of polarization effects. The coefficient 0.44 is a factor 1.36 below the value for hard spheres with elastic-specular collisions, according to the findings of Millikan.³⁴ The mobility diameter d is not the diameter d_s of the approximately spherical polymer globule, but is augmented by an effective gas molecule collision diameter: $d=d_s+d_g$.³⁵ The factor $(1-\beta\epsilon^*)$ in (1) is the polarization correction, where the constant β has been given previously as $\beta\approx 0.40$,³⁶ (for air at 20 °C, although it is thought to be independent of the nature of the gas and the temperature) and the parameter ϵ^* is defined as the ratio between the polarization energy at contact (α being the polarizability of the bath gas) and kT is the thermal energy. p is the gas pressure and $\mu = m_g m / (m_g + m)$ is the effective mass for ion-gas collisions (which for PEG ions of large mass m is very close to the molecular mass m_g of the gas molecules, and hence will be here approximated by m_g). Interestingly, ϵ^* and Z_o^2 have exactly the same dependence on z and d , so that one can write

$$\beta\epsilon^* = BZ_o^2, \quad (\text{SI-4})$$

where the coefficient B is completely defined by the previous expressions. Consequently,

$$Z = Z_o (1 - BZ_o^2). \quad (\text{SI-5})$$

Given experimentally measured Z , m/z and z , Z_o is obtained by inverting (SI-5), which from (SI-2) gives z/d^2 and therefore $d=d_s+d_g$. Since the polarization correction is small, we solve the cubic equation (SI-5) approximately via

$$Z_o \approx Z(1 + BZ^2). \quad (\text{SI-6})$$

This is not less accurate than the exact solution to the cubic equation (SI-5), but is rather consistent with the approximation of equation (SI-1), valid only in the limit $\epsilon^* \ll 1$.

Equation (SI-6) provides a fast algorithm to convert Z into Z_o , which complemented with our knowledge of z turns the horizontal variable of two-dimensional (2D) IMS-MS spectra such as that of Figure 2a into the mobility diameter $d=d_s+d_g$. The ordinate is similarly turned into the mass diameter, $d_m = (6m/\rho/\pi)^{1/3}$. Figure SI2 is a two dimensional spectrum of another PEG

³⁴ Millikan, R. A. *Phys. Rev.* **1923**, 22, 1–23.

³⁵ Tammet, H. J. *Aerosol Sci.* **1995**, 26, 459.

³⁶ Fernández-García, J.; Fernández de la Mora, J. *Measuring the Effect of Ion-Induced Drift-Gas Polarization on the Electrical Mobilities of Spherical, Multiply-Charged Ionic Liquid Nanodrops in Air*, submitted to *J. Am. Soc. Mass Spectrom.* 2013.

sample (PEG 6k) with the pairs ($1/Z$, m/z) converted into (d , d_m) variables. All these pairs fall right on top of the straight line $d=d_m+0.425$ nm, with the expected unit slope, and where the observed 0.425 nm shift is interpretable as the gas molecule diameter d_g for CO₂. Figure SI2 provides the first accurate measure available of d_g for CO₂, and the first confirmation that the coefficient β previously determined in air (considerably more carefully and accurately than here) is approximately applicable also to CO₂.

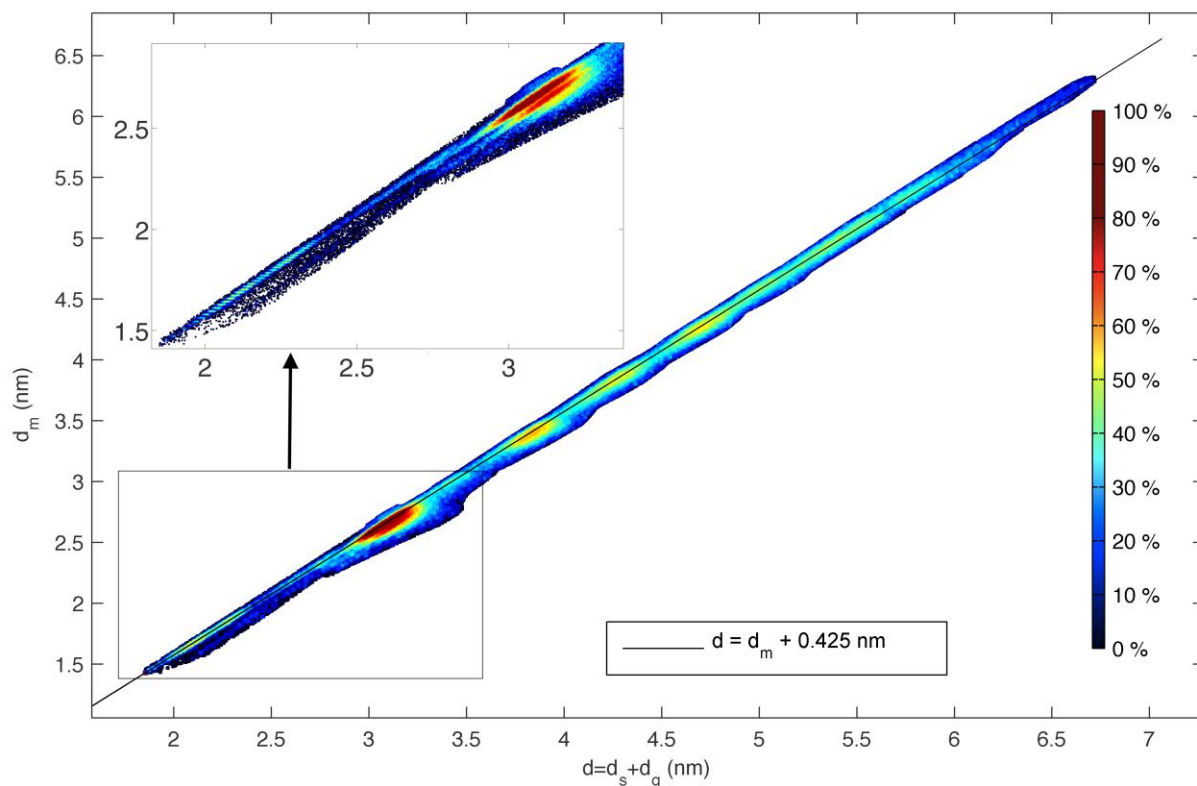


Figure SI2. Representation of the mass diameter versus the mobility diameter (corrected for polarization effects) for data similar to those of Figure 3b (taken for a sample of PEG 6k), and compared to the Stokes-Millikan curve for spheres.

Several anomalous groups of ions having lost one charge on their way to the vacuum system of the MS would not fall over the line $d=d_m+0.425$ nm unless one interpreted their m/z signal *correctly*, based on their z value at the DMA ($z_{DMA}=z_{MS}+1$). These unstable ions have been included in Figure SI2 with the *correct* interpretation.

SI.3. Analysis of narrow mass distribution PEG 12.6k

Figure SI3 shows an IMS-MS spectrum of PEG 12.6k sprayed in the negative mode in Methanol/Water (75/25 vol.) 30mM in Met₂AF. The main difference with the spectrum in Figure 2 of the main body of the article is the narrower mass distribution of this sample, enabling visual distinction of the various charge states z and levels of aggregation n of the ions, indicated in the form n^{+z} . Among the numerous high signal intensity regions (red) seen in Figure 2b, only the two most to the bottom (labeled 1^{-2} and 1^{-3}) and a weak low-mass tail labeled $z = -1$ are associated to a single chain of PEG 12.6 k. The other high intensity regions correspond to aggregates of several chains of PEG 12.6 k (dimer, trimer, ...), resulting from the high solution concentrations used (150 μ M). An aggregate of n monomers carrying z elementary charges will for brevity be denoted n^{-z} . The assignment of z is straightforward. The bands denoted $z=1$, $z=2$ and $z=3$ show well resolved mass peaks and are readily identified by the spacing of 44, 22 or 14.66 Da between subsequent peaks. This direct procedure fails at higher z and n , as the peaks become more blurred due to (i) the widening of the isotopic envelope, (ii) the shrinking of the spacing between oligomers (44/ z Da), (iii) the combination of n monomers with $2n$ end-groups (rather than just one monomer with 2 end-groups) in the mass region where more than one state of aggregation is present, (iv) the presence of more than one type of charging ion and other impurities. Nonetheless, the various bands are well separated, so that their corresponding z is simply given by their order, as indicated by the integer numbers on the right side of the figure.

Figure SI3 displays with particular clarity unstable ions, marked by the white arrow originating on 1^{-3} . This group corresponds to a fraction of the 1^{-3} ions having passed as such through the mobility analyzer, yet having lost an elementary charge on the entry path to the mass spectrometer, where they are mass analyzed as 1^{-2} . The similar transition $2^{-4} \rightarrow 2^{-3}$ and $3^{-5} \rightarrow 3^{-4}$ are also marked in the figure.

The IMS-MS spectrum of PEG 14k (Figure 2a) appears as far better resolved than in Figures SI3 and SI4. The difference is due to the presence in the narrow PEG 12.6k and 6k samples of a second low-abundance conformer of smaller mobility, which is absent from the broader PEG 14k sample. This interesting phenomenon is discussed in the following section.

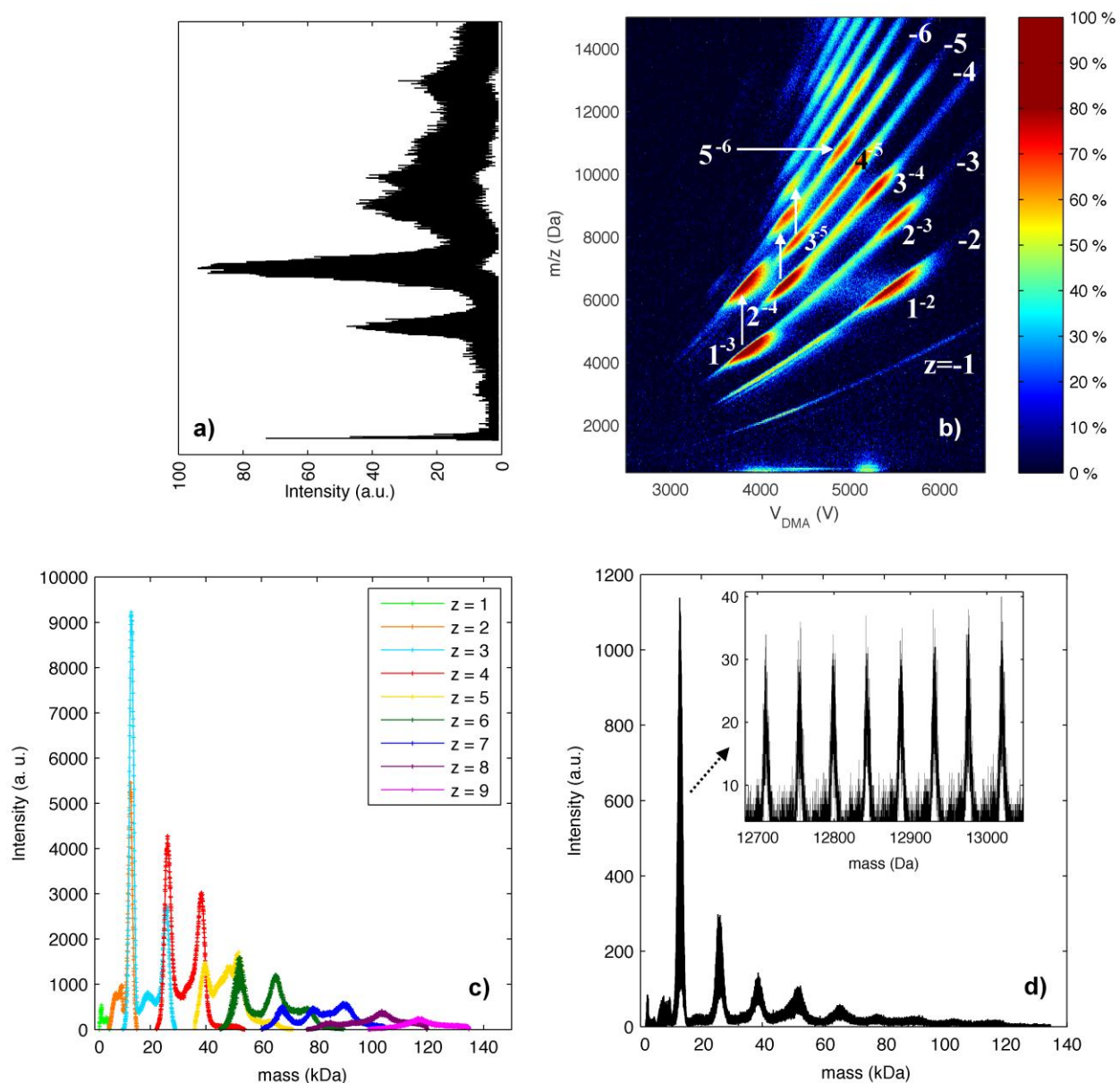


Figure SI3: Narrow mass distribution sample of PEG 12.6 kDa sprayed in the negative mode from 30mM Met₂AF in Methanol-Water (75:25 vol). (a): highly congested pure mass spectrum. (b): IMS-MS spectrum with annotation on the degree of agglomeration n and charge state z (n^{-z}). (c): z -resolved low-resolution ($\Delta m=44$ Da) mass distributions representing the ion counts $C_z(m_x)$ associated to ions composed of x CH₂-O-CH₂ linkers and carrying z formate ions. (d) Full-resolution distribution $f(x)$ given by summing full-resolution $C_z(m)$ data over all values of z .

SI.4. Multiple conformers

A most interesting feature of Figures SI3b and SI4a is the clear presence of several (primarily two) rather than just one mobility peak for given m and z . This is particularly clear in Figure SI4a for the lower masses on the $z = -2$ band. This complexity is relatively irrelevant from the analytical point of view, since most of the signal is associated to the most mobile conformer. However, the phenomenon is of basic interest and deserves some elaboration. Multiple conformers have not been previously discussed for the globular structure. They could not be recognized in our own earlier work,^{13, 8} probably because even the most favorable positive ionization buffers studied have yielded only a minute fraction of globular structures. Since the less mobile globular conformers provide a relatively weak signal even under our far more favorable conditions, they would have been difficult to distinguish from the noise in our earlier studies. Interestingly, Trimpin et al.³⁷ (Figure 1 C.2) have reported IMS-MS spectra clearly featuring several well defined conformers of PEG ions with structures intermediate between fully stretched and globular. Exceptionally, the globular branch of their $z = +2$ ions shows five well defined conformers spanning at given m a substantial range of mobilities ($Z_{\max}/Z_{\min}=1.11$). In contrast to our results, by far the most abundant of their isomers is the least mobile. One could tentatively attribute the observed range of conformations to the various positions that one or several charges could adopt in a long chain. However, there are many more such possible arrangements than conformations observed here. Accordingly, each of the few sharp experimental structures must necessarily include charges located at many different positions, so that these variations can have no measurable influence on the mobility. Close examination of this phenomenon for singly charged ions of a sample of PEG 2k (where the two conformers are much better resolved) shows that, at $m/z=2100$ Da, the second conformer line is shifted to smaller mobilities by the same amount as if one had added 9 linkers to the chain within the band of the first conformer. This is equivalent to a mass change of about 400 Da. Perhaps the mobility shift is due to attachment (nucleation in the source region) to some of the polymer ions of 4 dimethylammonium formate neutral ion pairs, which are then lost in the vacuum region of the MS. The hypothesis is congruent with the observation of more conformers (more nucleation) at higher charge states. However, this explanation seems improbable, due to the lack of adducts

³⁷ Trimpin, S.; Clemmer, D. E. Ion Mobility Spectrometry/Mass Spectrometry Snapshots for Assessing the Molecular Compositions of Complex Polymeric Systems, *Anal. Chem.* **2008**, *80*, 9073–9083.

formed by attachment of fewer (1, 2, 3) than these four presumed neutral ion pairs. The different mobilities found at the same mass may therefore correspond to different *phases* or arrangements in which the globule is able to organize itself. It is noteworthy that each of the z bands for each of the *phases* seen in Figure SI2 evolves continuously at increasing mass. The addition of one link to the polymer chain produces a continuous shift in mass, with no peculiarities (e.g. particularly large or small mobilities) associated to a given (magic) number of monomers. This may appear as a trivial observation, but the same is not true for clusters of crystalline solids as the number of identical constituent molecules increases. It is however true for clusters of materials such as ionic liquids, which are liquid in bulk form.^{26,28} The z -bands so far observed for ionic liquid clusters show only one conformer. This suggests that these small PEG ions are liquid-like or glassy, and form more than one phase. Interestingly, the inset of Figure SI2 shows that these phases continue each other across different values of z . For instance, the red region in the inset displays clearly two conformers (and even a weaker third one) for the doubly charged ions. The most intense and mobile conformer is extended smoothly at small masses by the weak signal associated to singly charged ions, and so does the third, even less mobile conformer, although the signal for the singly charged ions of this conformer is very weak.

SI.5. Charging probability at low z captured with PEG 6k

The rising side of the $z = 2$ curve is barely captured by the $p_2(m)$ data of Figure 2d, as the corresponding low masses are on the very edge of this sample. This region has been studied with a lower molecular weight sample (the same PEG 6k used for Figure SI2), with results shown in Figure SI4.

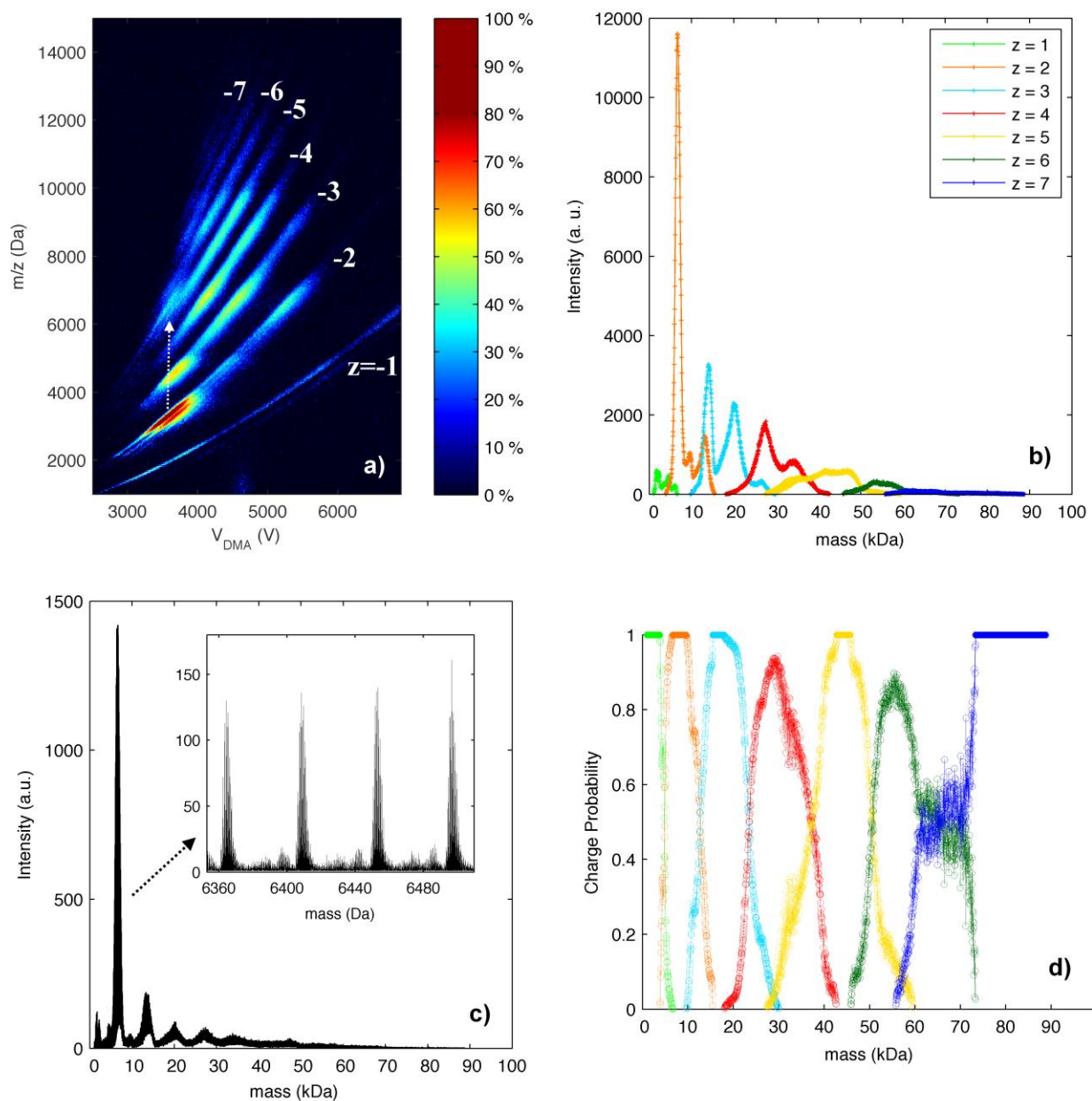


Figure SI4: Analysis of a sample of PEG 6k sprayed in the negative mode from a solution of 30mM Met₂AF in Methanol/Water (75/25 vol). (a) IMS-MS spectrum. (b) Low resolution ($\Delta m=44$ Da) charge-resolved abundance distributions $C_z(m_x)$. (c) Mass distribution (full resolution in the inset), with peaks from left to right corresponding to $n = 1, 2, \dots$ (d) Low resolution charge distribution $p_z(m_x)$ as defined in (9)

SI.6. More on the ionization mechanism

In reinforcement of the ion evaporation mechanism defended in the main body of the article, consider for instance the curve for $z = 6$ in Figure 2d. A chain with $m=73$ kDa has close to 100% probability of holding these 6 charges. As the polymer ion size is reduced, the field on its surface increases, the activation energy for ion evaporation decreases, and ion evaporation begins to proceed at a measurable rate, so that an observable fraction of these ions lose one charge. The process continues through a narrow range of decreasing masses, until all the ions carry just 5 charges. If one now considers PEG ions with an increasing mass above 73 kDa, all will be able to hold the 6 charges. However, the number of those holding 6 charges diminishes rapidly with increasing size because these ions had initially many more charges than 6, so they will retain as many as allowed by the ion evaporation mechanism. In other words, the same mechanism that defines the rising tail of the $z = 6$ curve and the related dropping tail of the $z = 5$ curve repeats itself at every charge state.

Table SI1. Minimum mass $m_{min}(z)$ observed for the different charge states z present in various PEG samples, compared to that for the smallest globule able to hold z charges, $m^*(z) \sim 0.5 z^2$

z		2	3	4	5	6	7	8	9
$m^*(z) = 0.5 z^2$ (kDa)		2.0	4.5	8.0	12.5	18.0	24.5	32.0	40.5
$m^*(z) = 0.635 z^2$ (kDa)		-	-	-	15.9	22.9	31.1	40.6	51.4
$m_{min}(z)$ (kDa)	PEG 6k	3.7	9.9	17.9	28.1	46.0	55.3	-	-
	PEG 12.6k	5.1	10.1	22.3	36.0	45.2	60.1	76.3	98.5
	PEG 14k	-	11.2	21.3	38.0	53.5	66.2	87.0	108.2

SI.7. DMA-MS analysis at reduced PEG concentration

The high PEG concentrations used so far are useful to enhance the signal and to produce aggregates, widening the mass range available for our studies from a small number of PEG samples. However, in practical mass analysis one needs to use samples sufficiently diluted to minimize the production of aggregates that would otherwise distort the true mass distribution. Accordingly, to assess the analytical relevance of our approach, we have examined several samples at lower PEG concentrations, down to 10 μ M. These tests have used the same buffer as

before: 30mM Met₂AF in Methanol-Water (75:25 vol.). The results, shown in Figures SI5, demonstrate an incomplete but still considerable reduction of clustering, with only the monomer and a modest proportion of dimer appearing in all the samples tested at these lower concentrations. To improve the evaporation of the electrospray droplets and favor the signal intensity measured by the mass spectrometer, a co-flow of about 2 liters per minute heated up to some 50 °C was passed through the electrospray chamber. Note in the top left figure (for PEG 12.6k) the appearance of peaks beyond the $z = 4$ line. As indicated with white arrows, these are not due to higher states of aggregation beyond $n = 2$, but to charge loss transitions (occurring after the mobility measurement) originating from 1^{-3} and 2^{-4} , respectively.

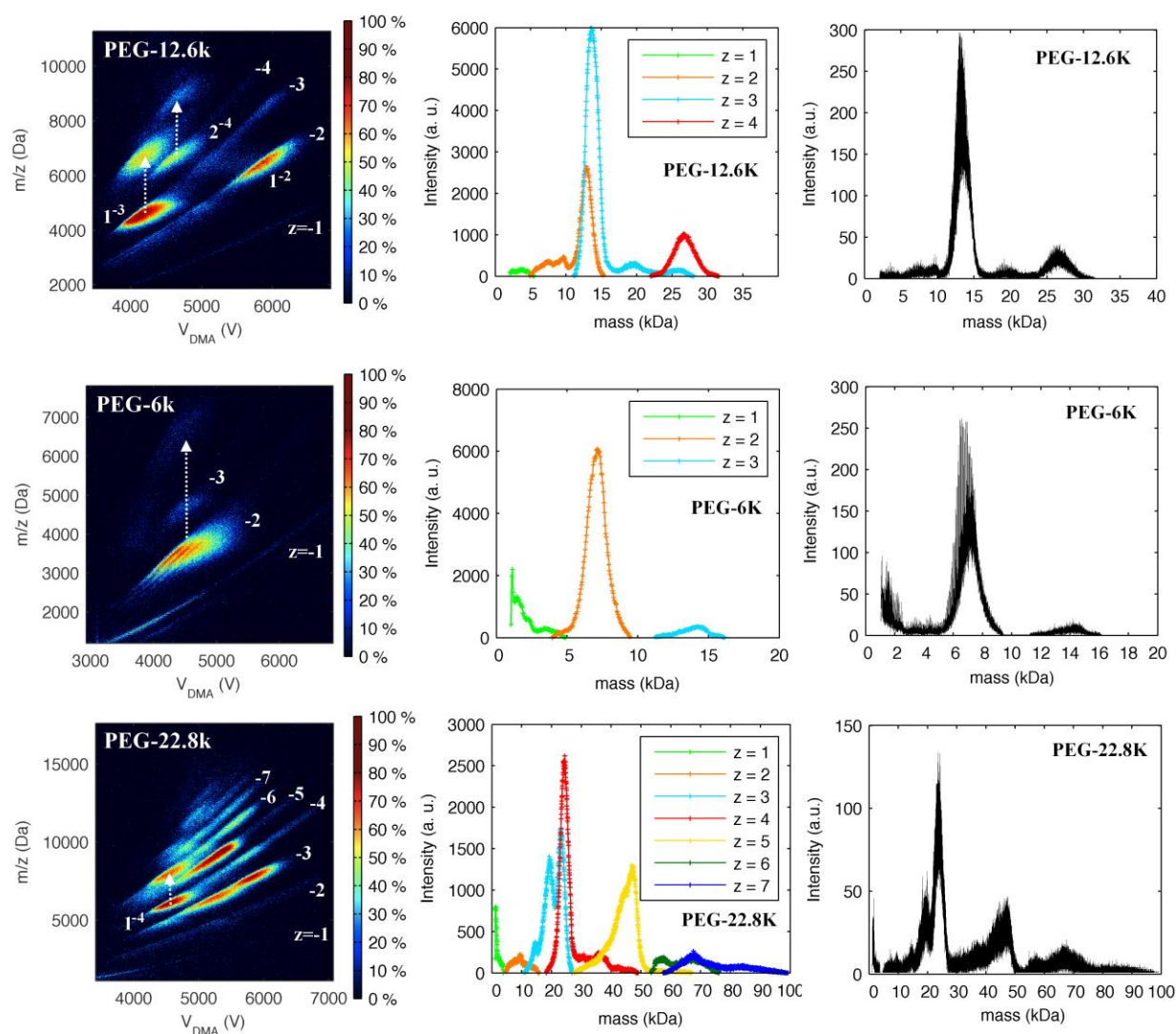


Figure SI5. Analysis of PEG samples at reduced concentrations; negative mode; 30mM Met₂AF in Methanol-Water (75:25 vol.). Left: IMS-MS spectra; Center: charge-resolved abundance distributions $C_z(m_x)$; Right: Full resolution mass distributions. From top to bottom: 10 μ M PEG 12.6k; 10 μ M PEG 6k; 25 μ M PEG 22.8k

SI.8. Studies with PEG 2k

This sample was examined to extend the available information on ionization probability to relatively small sizes. As shown in Figure SI6, a dominant series of singly charged ions spaced by 44 Da extends down to a mass of at least 767.7 Da, including weaker members down to 547.5 Da. Within the error associated to lack of calibration of the MS (0.23 Da), this series corresponds to PEG attached to formate. The dominant series of singly charged ions seen in this sample starts above the peak at 1354.91 Da and is attached to a different anion (shifted to the left by ~29 Da). Notice also the clear existence in this sample of several conformers having exactly the same mass.

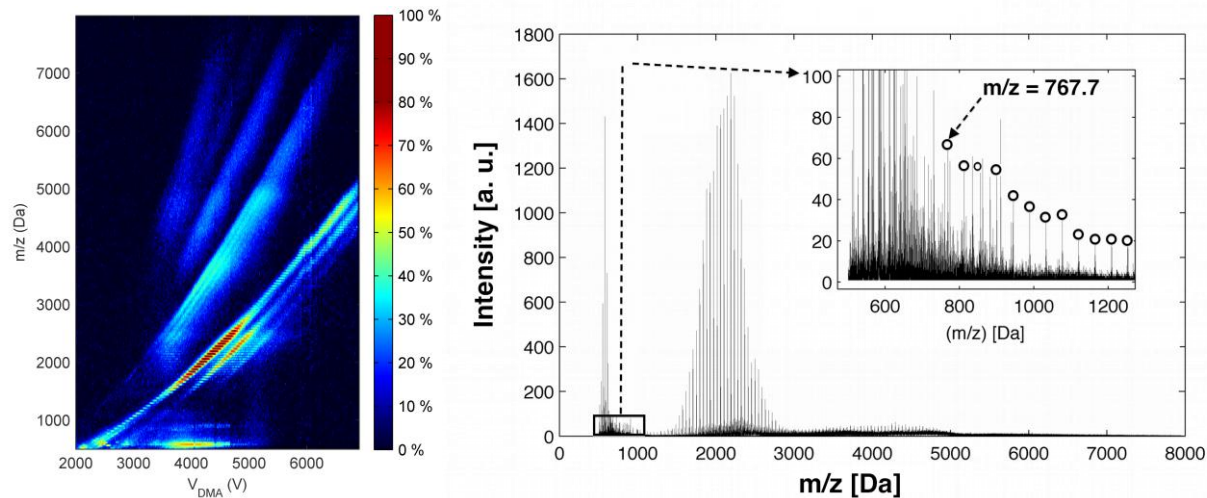


Figure SI6: Spectra for a sample of PEG 2k. Left, DMA-MS spectrum. Right, pure mass spectrum, with an inset zooming on the low masses and marking with circles a dominant sequence of peaks spaced from each other by 44 Da.